ONCOIMMUNOLOGY
2016, VOL. 5, NO. 8, e1208878 (10 pages)
http://dx.doi.org/10.1080/2162402X.2016.1208878

Taylor & Francis
Taylor & Francis Group

ORIGINAL RESEARCH

Nitric oxide synthase 2 is involved in the pro-tumorigenic potential of γδ17 T cells in melanoma

Laetitia Douguet[a,b,c], Lloyd Bod[a,b,c,*], Renée Lengagne[a,b,c,*], Laura Labarthe[a,b,c,d], Masashi Kato[e], Marie-Françoise Avril[a,b,c,f], and Armelle Prévost-Blondel[a,b,c]

[a]Institut National de la Santé et de la Recherche Médicale (INSERM), U1016, Institut Cochin, Paris, France; [b]Centre National de la Recherche Scientifique (CNRS), UMR8104, Paris, France; [c]Université Paris Descartes, Sorbonne Paris Cité, Paris, France; [d]Ecole Normale Supérieure, Cachan, France; [e]Nagoya University Graduate School of Medicine, Nagoya, Aichi, Japan; [f]Cochin Hospital, Paris, France

ABSTRACT

γδ T lymphocytes may exert either protective or tumor-promoting functions in cancer, mostly based on their polarization toward interferon (IFN)-γ or interleukin (IL)-17 productions, respectively. Here, we demonstrate that γδ T cells accelerate the spontaneous metastatic melanoma development in a model of transgenic mice for the human RET oncogene (Ret mice). We identify unanticipated roles of inducible nitric oxide synthase (NOS2) in favoring the recruitment of pro-tumor γδ T cells within the primary tumor. γδ T cells isolated from Ret mice deficient for NOS2 produced more IFNγ and less IL-17 than their counterparts from Ret mice. By supporting IL-17 production by γδ T cells, NOS2 leads to the recruitment of polymorphonuclear myeloid-derived suppressor cells (PMN-MDSCs) and metastasis formation. NOS2 also reduces the cytotoxicity of γδ T cells toward melanoma cells. Finally, we detected NOS2 expressing γδ T cells in the primary tumor and tumor-draining lymph nodes in Ret mice, but also in human melanoma. Overall our results support that this NOS2 autocrine expression is responsible for the polarization of γδ T cells toward a pro-tumor profile.

ARTICLE HISTORY
Received 3 June 2016
Revised 24 June 2016
Accepted 27 June 2016

KEYWORDS
Interleukin 17; melanoma; NOS2; pro-tumor functions; γδ T cells

Introduction

Following the first evidence provided by Hayday and colleagues that γδ T lymphocytes play a key role in tumor immunosurveillance of cutaneous malignancies,[1] several reports highlighted the protective properties of γδ T lymphocytes during tumor progression (reviewed in ref.[2]). Recently, the tumor-associated γδ T cell specific signature emerged as the most significant favorable cancer-wide prognostic immune population in a meta-analysis of human malignancies.[3] The antitumor properties of γδ T cells rely on their capacity to directly lyse tumor cells and produce interferon-γ (IFNγ).[4] Interleukin (IL)-17 producing γδ T cells (γδ17) have more rarely been involved in tumor elimination, e.g., following immunogenic anthracycline-based therapy and radiotherapy,[5] or in models of microbiota-associated tumor control.[6,7] Contrasting with these studies, recent data reveal that the presence of γδ T lymphocytes correlates with tumor severity in human breast and colon cancers.[8] The tumor-promoting properties of γδ T lymphocytes are mainly attributed to their ability to secrete IL-17. Indeed, γδ17 cell-derived IL-17 leads to the recruitment of myeloid-derived suppressor cells (MDSCs) that favors tumor immune escape and metastasis (reviewed in ref.[9]).

The nitric oxide synthase 2 (NOS2) is the inducible form of a family of three isoenzymes that catalyzes the production of nitric oxide (NO) from the amino-acid arginine. Endogenous NOS2 expression has recently been discovered in both mouse and human $CD4^+$ T cells producing IL-17 (Th17).[10,11] Autocrine NOS2 inhibited the polarization of murine Th17,[10] whereas it was required for inducing and maintaining the Th17 phenotype of human $CD4^+$ T lymphocytes.[11] While local microenvironment may contribute to the anti or pro-tumor polarization of γδ17 cells, we investigated the role of NOS2 in this process. Here, we report that NOS2 expression by γδ T cells improves their pro-tumor functions in melanoma.

Results

NOS2 deficiency delays tumor cell dissemination in melanoma

Ret mice develop spontaneously metastatic melanoma due to transgenic expression of a constitutively activated form of the human RET oncogene.[12-14] To address the role of NOS2 in the tumor development, we set up a new Ret model in which NOS2 is genetically inactivated (RetNos2KO mice). 50% of RetNos2KO mice developed a primary melanoma at day 67, whereas the median time for tumor detection in Ret mice was day 38 (Fig. 1A). Nevertheless, more than 80% of both groups exhibited a primary tumor at 6 mo indicating that NOS2 deficiency does not block tumor formation, but rather delays the primary tumor onset (Fig. 1A). NOS2 inactivation also slows

CONTACT Armelle Prévost-Blondel armelle.blondel@inserm.fr Institut Cochin, 22 rue Méchain, 75014, Paris, France.
Supplemental data for this article can be accessed on the publisher's website.
*These authors contributed equally to this work.

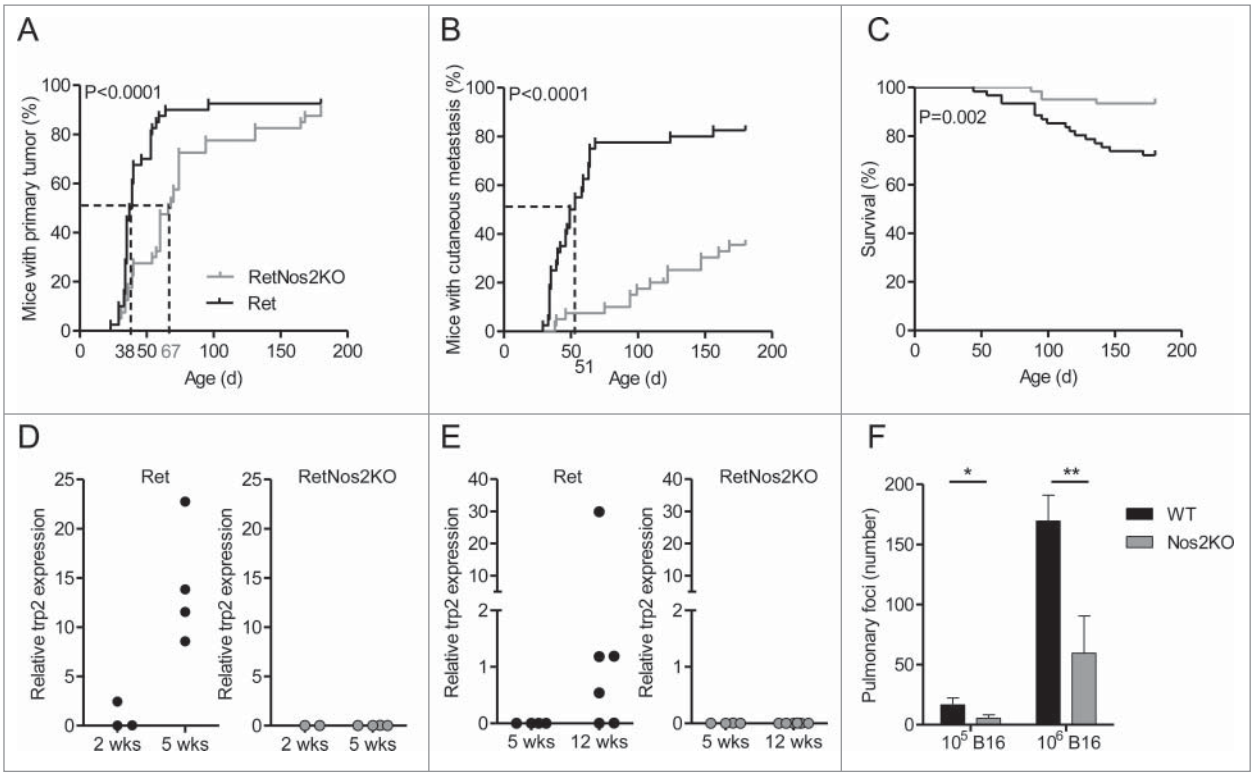

Figure 1. NOS2 deficiency delays melanoma progression by inhibiting tumor cell dissemination (A–C) 6-mo follow-up of melanoma development from Ret (n = 40) and RetNos2KO (n = 40) mice. (A,B) Time courses of primary tumor and cutaneous metastasis onset. Mice were examined every 2 weeks. (C) Survival curve. (Mantel-Cox test (A–C)). (D, E) trp2 expression was measured by qRT-PCR in bladders (D) and tumor dLNs (E) collected from Ret and RetNos2KO mice aged of 2, 5 or 12 weeks. Expressions were normalized using GAPDH. Each point represents one mouse. (F) Number of pulmonary metastasis in WT mice and Nos2KO mice after i.v. injections of 10^5 (n = 8 WT, n = 9 Nos2KO) or 10^6 (n = 6 per group) B16 melanoma cells. Data are pooled from two independent experiments (mean ± SEM) (Mann–Whitney test). $^{*}p < 0.05$, $^{**}p < 0.01$.

down tumor cell dissemination at skin and distant sites (Fig. 1B and Table S1) and accordingly significantly improves the mouse survival in our model (Fig. 1C). The presence of micro-metastases were detected, by the analysis of trp2 and tyrosinase expression, in the bladder and tumor-draining lymph nodes, two of the most frequent metastatic sites, in 5 and 12 week old Ret mice, respectively (Figs. 1D and E and S1). In striking contrast, no micro-metastasis was found in RetNos2KO mice suggesting a delay of metastasis formation in these mice. Of note, Nos2 deficient (Nos2KO) mice also exhibited less lung foci than wild-type (WT) mice (Fig. 1F) 14 d after B16 melanoma cell inoculation intravenously. Together our data show that the NOS2 deficiency delays tumor cell dissemination in two melanoma models.

NOS2 deficiency decreases PMN-MDSCs infiltration within primary tumors

It is well established that NOS2 derived from MDSCs inhibits antitumor response mediated by $\alpha\beta$ T lymphocytes.[15] NOS2 inactivation could directly contribute to the better tumor control observed in RetNos2KO mice by restoring cytolytic properties of T cells. To evaluate whether the global immunosuppression is reduced in Nos2 deficient mice, we used an *in vivo* cytolysis assay (Fig. S2). The lysis of specific target cells was similar in WT and Nos2KO mice (left panels). Target cells were also lysed with the same efficacy in WT and Nos2KO tumor-bearing mice (right panels), indicating that NOS2 inactivation does not significantly enhance the cytolytic ability of $\alpha\beta$ $CD8^+$ T cells.

Next, we investigated whether the more efficient tumor control in RetNos2KO mice relies on a specific tumor microenvironment. We analyzed *ex vivo* cytokine profiles in primary tumors derived from 6-mo animals. The protein levels of IL-12p70, IFNγ, IL-10, and tumor necrosis factor-α (TNF-α) were quite similar in both groups (Fig. 2A). Vascular endothelial growth factor (VEGF) was statistically more abundant in Ret mice (Fig. 2A) than in RetNos2KO mice consistent with the higher tumor cell dissemination (Figs. 1B, D, and E). Tumors from Ret mice contained also higher amounts of keratinocyte-derived cytokine (KC), a murine IL-8 homolog involved in PMN recruitment, and granulocyte colony stimulating factor (G-CSF), a key regulator in PMN biology. IL-17 was upregulated when NOS2 was functional, as well as IL1-β and IL-6 both known to stimulate IL-17 production from $\alpha\beta$ T lymphocytes, (Fig. 2A). We next quantified the immune cells that infiltrate primary tumors. Such global analysis revealed a huge redistribution in the ratio of myeloid versus lymphoid cells. Primary tumors from RetNos2KO mice exhibited significantly less proportion of myeloid cells than primary tumors from Ret mice (48% vs. 64%) (Fig. 2B). Detailed analysis of myeloid population disclosed no difference in the proportions and absolute numbers of dendritic cells (DC), macrophages and monocytic MDSCs (M-MDSCs) among haematopoietic cells. In striking contrast, but concordant with KC and G-CSF quantification, PMN-MDSCs poorly infiltrated primary tumors in RetNos2KO

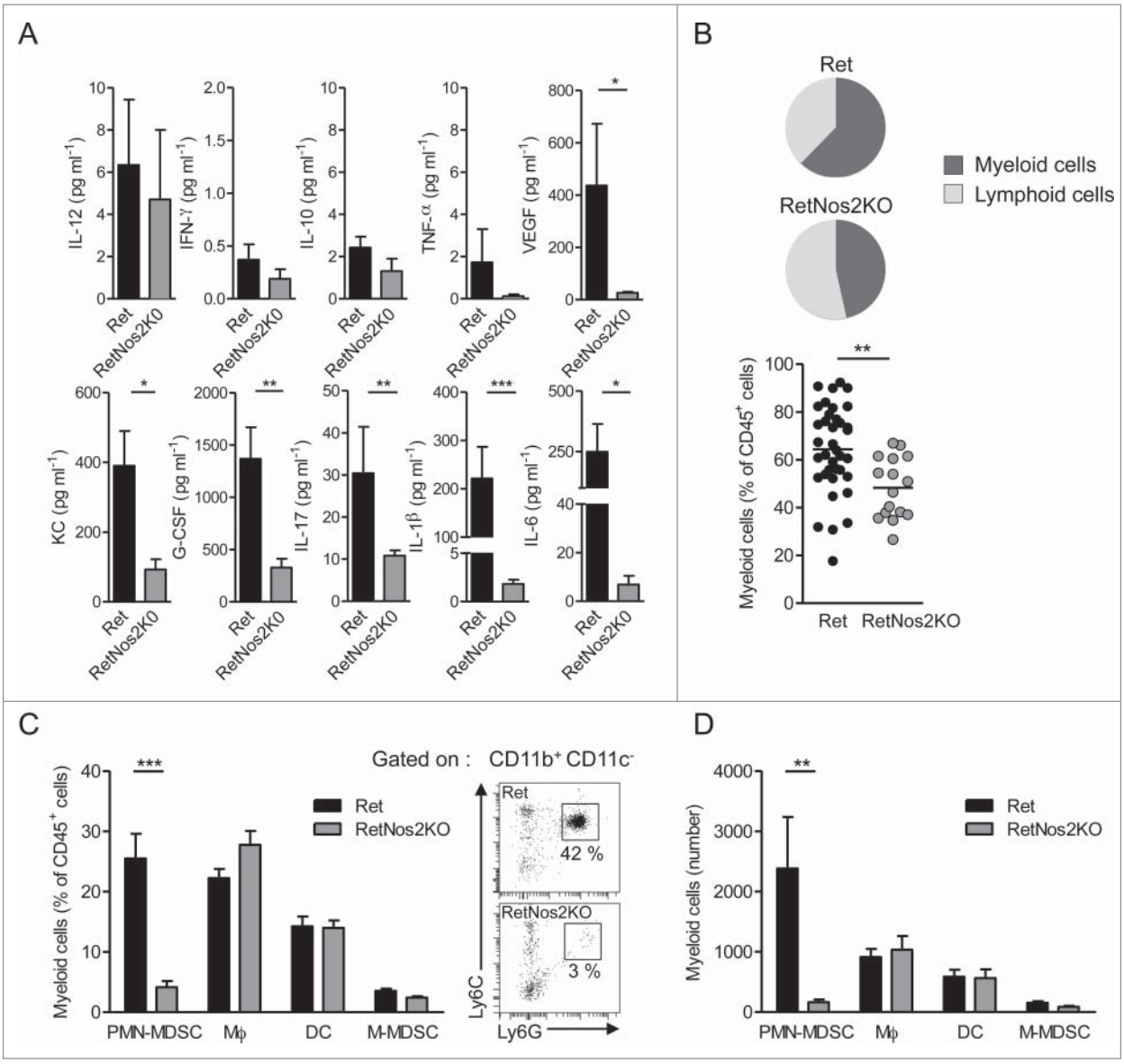

Figure 2. NOS2 deficiency reduces PMN-MDSCs infiltration in primary tumors (A) Protein levels of indicated cytokines in primary tumors, from Ret (n = 14, except for G-CSF n = 11, IL-17 n = 10 and VEGF n = 8) and RetNos2KO (n = 8, except for IL-17 n = 6) mice, determined by ELISA and multiplex ELISA. (B) Proportions of myeloid cells among $CD45^+$ cells within primary tumors of Ret (n = 35) and RetNos2KO (n = 16) mice (C,D) Dendritic cells (DC: $CD11c^+$), macrophages (MΦ: $CD11b^+CD11c^-Ly6C^{-/low}Ly6G^-$), monocytic MDSCs (M-MDSCs: $CD11b^+CD11c^-Ly6C^{high}Ly6G^-$) and PMN-MDSCs ($CD11b^+CD11c^-Ly6C^{low}Ly6G^+$) were analyzed by flow cytometry. Percentages (C) and absolute numbers (D) of myeloid cell subsets within primary tumors of Ret (n = 35) and RetNos2KO (n = 16) mice are shown (left). Representative dot plots of PMN-MDSCs staining (right), Data are pooled from at least three independent experiments. Each point represents individual mouse. Bars are mean ± SEM. $^*p < 0.05$, $^{**}p < 0.01$ $^{***}p < 0.001$ (Mann–Whitney test).

mice compared to Ret mice (Figs. 2C and D). Taken together, a weaker recruitment of this immunosuppressive population, known to play a key role in tumor cell dissemination in the Ret model,[16] may account for resistance to tumor development in RetNos2KO mice.

NOS2 supports IL-17 production by γδ T cells

Recent data strongly support the essential contribution of IL-17-producing γδ T cells in PMN-MDSCs recruitment.[17-19] We compared the proportion of tumor-infiltrating γδ T cells in Ret and RetNos2KO mice. While NOS2 deficiency leads to an increased proportion of lymphoid cells in primary tumor (Fig. 2B), γδ T cells were twice less abundant in Ret mice deficient for NOS2 (Fig. 3A). Interestingly, when NOS2 is functional, a positive correlation between the numbers of tumor-infiltrating γδ T cells and PMN-MDSCs is observed, which is absent in RetNos2KO mice (Fig. 3B). These results suggest that γδ T cells contribute to the recruitment of PMN-MDSCs in primary melanoma. Consequently, we pursued this study by focusing on IL-17 production. As we observed above in Fig. 2A, NOS2 promotes an inflammatory microenvironment within the primary tumor, which supports IL-17 production. We performed *ex vivo* intracellular stainings to identify tumor-infiltrating IL-17-producing populations in our model. Immune cells from primary tumors of Ret mice globally produced more IL-17 compared with their counterparts from RetNos2KO mice (Fig. 3C). Among IL-17-producing cells, percentages and absolute numbers of γδ T cells were much more substantial than those of $CD4^+$ T cells (Figs. 3D and E),

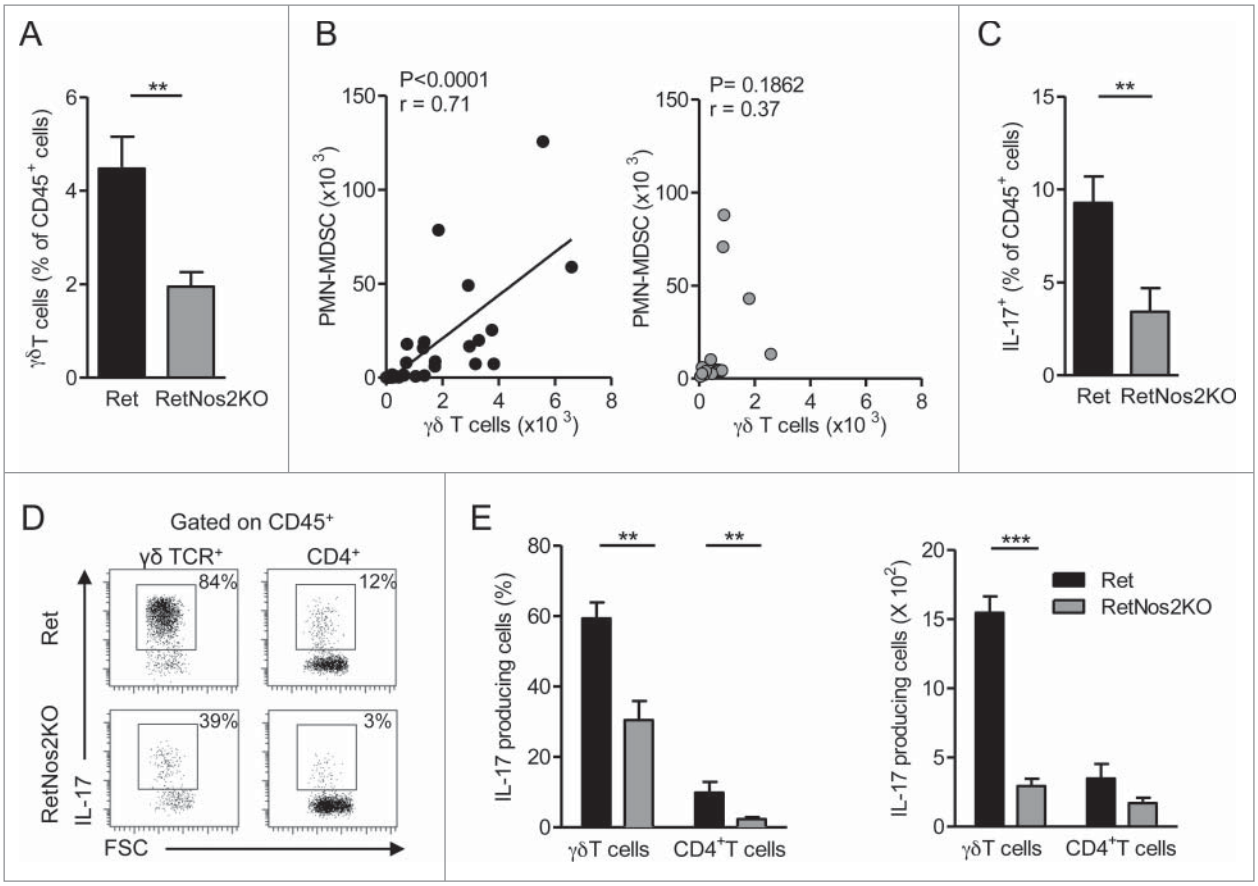

Figure 3. NOS2 deficiency decreases IL-17-producing $\gamma\delta$ Tcells (A) Percentage of $\gamma\delta$ T cells among CD45$^+$ cells in primary tumors of Ret (n = 9) and RetNos2KO mice (n = 11). (B) Correlation between the numbers of $\gamma\delta$ T cells and PMN-MDSCs within the primary tumors of Ret (n = 33) (left) and RetNos2KO (n = 17) (right) mice. Each point represents individual mouse and line is linear regression. (C–E) IL-17 production assessed by flow cytometry on single-cell suspensions derived from primary tumors of Ret (n = 11) and RetNos2KO mice (n = 10) after PMA/ionomycin stimulation. (C) Percentage of total IL-17producing CD45$^+$ cells. (D) Representative FSC/IL-17 dot plots are shown for $\gamma\delta$ T cells and CD4$^+$ T cells. (E) Percentage (left) and absolute number (right) of $\gamma\delta$ T cells and CD4$^+$ T cells producing IL-17. Bars are mean ± SEM. $^*p < 0.05$, $^{**}p < 0.01$, $^{***}p < 0.001$ (Mann–Whitney test A, C–E and Pearson correlation test B).

indicating that $\gamma\delta$ T cells are the main source of IL-17 in our models. Moreover, nearly 60% of them produce IL-17 in Ret mice, whereas only 30% exhibit this capacity in RetNos2KO mice. Thus, NOS2 inactivation significantly reduces the pool of $\gamma\delta$17 cells infiltrating primary tumors. Similar results were observed in tumor-draining lymph nodes (Fig. S3A) and prompted us to investigate whether the tumor microenvironment is the only stimulus involved in the polarization of $\gamma\delta$ T cells into IL17 producers. Unexpectedly, we found that $\gamma\delta$17 cells derived from peripheral LNs (pLNs) were already more frequent in WT mice than in Nos2KO mice (Fig. S3B). CD27 expression is known to segregate two peripheral functional subsets of $\gamma\delta$ T cells. CD27$^+$ $\gamma\delta$ T cells display Th1 characteristics including intracellular IFNγ, whereas most of CD27$^-$ $\gamma\delta$ T cells produce IL-17.[20] In agreement with their enhanced IL-17 production, we found a higher proportion of CD27$^-$ $\gamma\delta$ T cells in WT mice compared to Nos2KO mice (Fig. S3C). This discrepancy was observable in both Vγ1$^+$ and Vγ4$^+$ T cells that represent the two main peripheral $\gamma\delta$ T cell subsets (Fig. S3D).

Collectively, our data demonstrate that NOS2 deficiency limits the pool of tumor-infiltrating $\gamma\delta$ T cells, in particular $\gamma\delta$17 that may support the poor recruitment of PMN-MDSCs within the primary tumor of RetNos2KO mice. These results further highlight that NOS2 promotes $\gamma\delta$17 cell polarization independent of the tumor context through regulating the balance between CD27$^+$/CD27$^-$ $\gamma\delta$ T cell subsets.

NOS2 enhances pro-tumor properties of $\gamma\delta$ T cells

We next investigated how NOS2 affects the functions of $\gamma\delta$ T cells toward tumors. We compared the ability of $\gamma\delta$ T cells derived from Ret or RetNos2KO mice to lyse B16 melanoma cells *in vitro* over a 4-h period (Figs. 4A and B). Both sources of $\gamma\delta$ T cells after a sub-optimal TCR stimulation had no significantly impact on the B16 melanoma cell index (Fig. 4A). After TCR triggering, $\gamma\delta$ T cells significantly decreases the B16 cell index (Fig. 4B). But $\gamma\delta$ T cells from RetNos2KO mice lysed tumor cells more efficiently than their counterparts derived from Ret mice (Fig. 4B). Consistent with direct quantification of IFNγ in primary tumors of Ret and RetNos2KO mice (Fig. 2A), we found similar proportions of IFNγ-producing cells among haematopoietic cells after PMA/ionomycine stimulation (Fig. 4C). Nevertheless, tumor-infiltrating $\gamma\delta$ T cells able to produce IFNγ are more abundant in RetNos2KO mice than in Ret mice (Fig. 4D). Taken with IL-17 data, these results show that NOS2 favors pro-tumor properties of $\gamma\delta$ T cells.

To directly assess the contribution of $\gamma\delta$ T cells to melanoma progression in our model, we set up Ret mice deficient

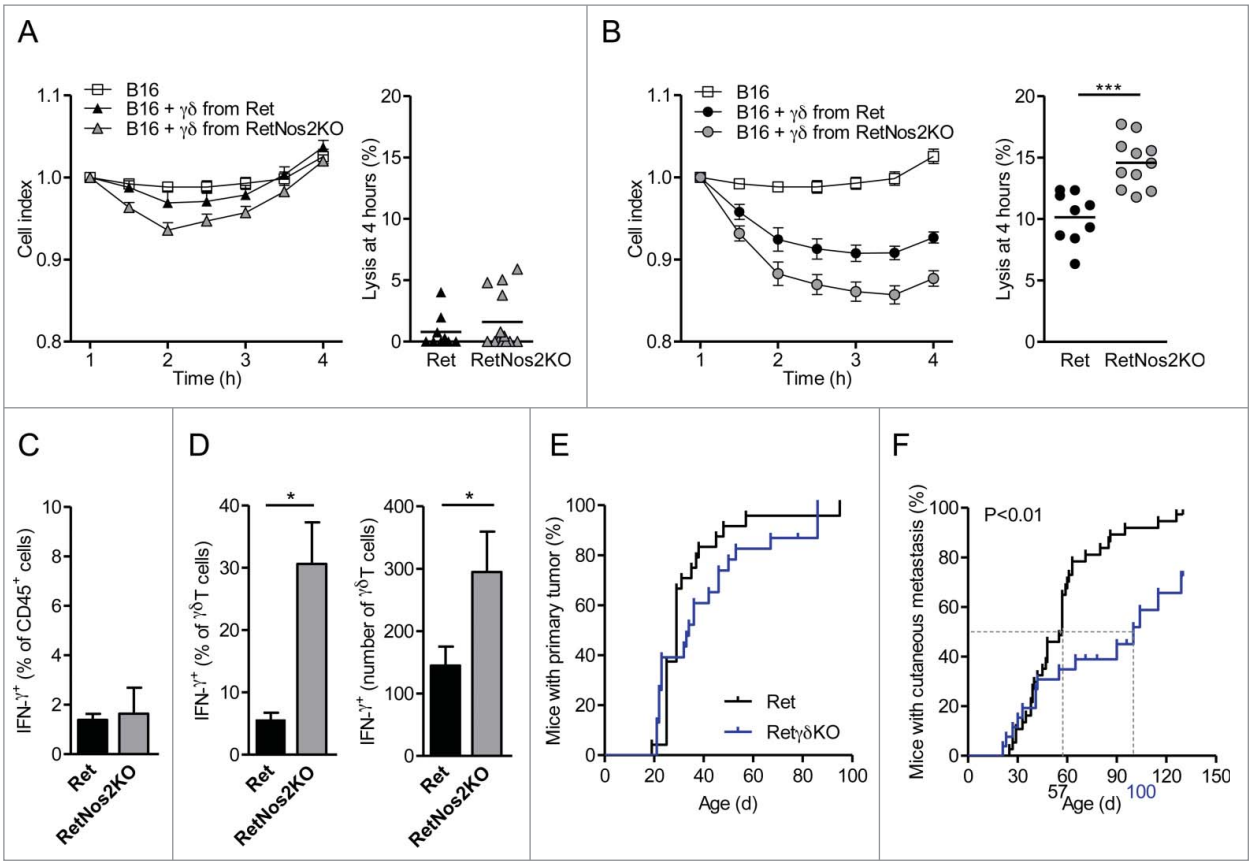

Figure 4. NOS2 improves pro-tumor properties of $\gamma\delta$ Tcells. (A, B) Cytotoxic activity of $\gamma\delta$ T cells derived from Ret and RetNos2KO mice. B16 cells were seeded in wells of E-plates. $\gamma\delta$ T cells stimulated with anti-CD28 (A) or anti-CD3 plus anti-CD28 (B) were added to a ratio of one $\gamma\delta$ T cell for two B16 cells (see Methods). The inhibition of tumor cell proliferation was assessed by dynamically monitoring every 30 min on cell impedance. The graph (left) shows the normalized cell index values. The percent of B16 melanoma cell lysis (right) was calculated 4 h after addition of effector cells. Data are pooled from two independent experiments with 9 (non-stimulated and stimulated Ret), 11 (stimulated RetNos2KO) and 13 (non-stimulated RetNos2KO) replicates. (C,D) IFNγ production assessed by flow cytometry on single-cell suspensions derived from primary tumors of Ret (n = 5) and RetNos2KO mice (n = 4) after PMA/ionomycin stimulation. (C) Percentage of total IFNγ producing CD45$^+$ cells. (D) Percentage (left) and absolute number (right) of $\gamma\delta$ T cells producing IFNγ. (E,F) 4-mo follow-up of melanoma development from Ret (n = 37) and Ret$\gamma\delta$KO (n = 26) mice. Time courses of primary tumor (F) and cutaneous metastasis (F) onset. Mice were examined every 2 weeks. Data are mean ± SEM. ((A)and (B) left, C,D) except mean ((A) and (B) right). Each point represents one replicate ((A)and (B) right). $^*p < 0.05$, $^{***}p < 0.001$ (Mann–Whitney test (A–C) and Mantel-Cox test (E,F)).

for $\gamma\delta$ T cells (Ret$\gamma\delta$KO) and followed the tumor development in these mice (Figs. 4E and F). Despite similar primary tumor onsets in Ret and Ret$\gamma\delta$KO mice (Fig. 4D), cutaneous metastasis developed later in Ret$\gamma\delta$KO mice than in Ret mice (Fig. 4F). Indeed, 50% of Ret mice had a cutaneous metastasis at day 57, whereas the median time for metastasis detection was day 100 in Ret$\gamma\delta$KO mice (Fig. 4F). Cutaneous metastases are also less frequent in Ret$\gamma\delta$KO mice (Fig. 4F). This data demonstrates the pro-tumor role of $\gamma\delta$ T cells in our model. Nevertheless, the tumor protection conferred by the absence of $\gamma\delta$ T cells is less efficient than in case of NOS2 deficiency (Figs. 1A and B). Consequently, we analyzed the production of IL-17 in Ret$\gamma\delta$KO mice. We quantified similar amount of IL-17 in primary tumors derived from 4-mo Ret and Ret$\gamma\delta$KO mice (Fig. S4A). Accordingly, TdLNs from Ret and Ret$\gamma\delta$KO mice display similar proportion of IL-17-producing immune cells after PMA/ionomycin stimulation (Fig. S4B). CD4$^+$ T and CD8$^+$ T cells in absence of $\gamma\delta$ T cells are able to produce more IL-17 than in Ret mice as revealed by percentages and absolute numbers of IL-17 producing cells (Figs. S4C and D). Taken together our data show that CD4$^+$ T and CD8$^+$ T cells compensate the absence of IL-17-producing $\gamma\delta$ T cells and could explain partial protection observed in Ret$\gamma\delta$KO mice. In addition, these results highlighted the relative contribution of IL-17 in our model.

$\gamma\delta$ T cells infiltrating melanomas in mice and human display the capacity to express NOS2

All our data prompted us to investigate whether the action of NOS2 on $\gamma\delta$ T cell properties is due to their own capacity to produce this enzyme. About 25% of $\gamma\delta$ T cells were found to express NOS2 in primary tumors (not shown) and in TdLNs of Ret mice (Fig. 5A). This autocrine expression may directly induce the polarization of $\gamma\delta$ T cells toward a pro-tumor phenotype.

Finally, we addressed the relevance of this finding in human biopsies. A total of 14 primary tumors were collected from melanoma patients. According to Breslow thickness, there were three groups of patients with various risks of disease's relapse: three patients in a low risk group (melanoma < 1 mm), three patients in an intermediate risk group (1.01 mm < melanoma < 2.99 mm) and eight patients in a high risk group (melanoma > 3 mm). The clinical data and results of immunofluorescence analyses are summarized in Table S2. An arbitrary cut-off for the number of $\gamma\delta$ T cells per microscopic field was used to define tumors as highly (+++ to ++) or weakly (+) infiltrated

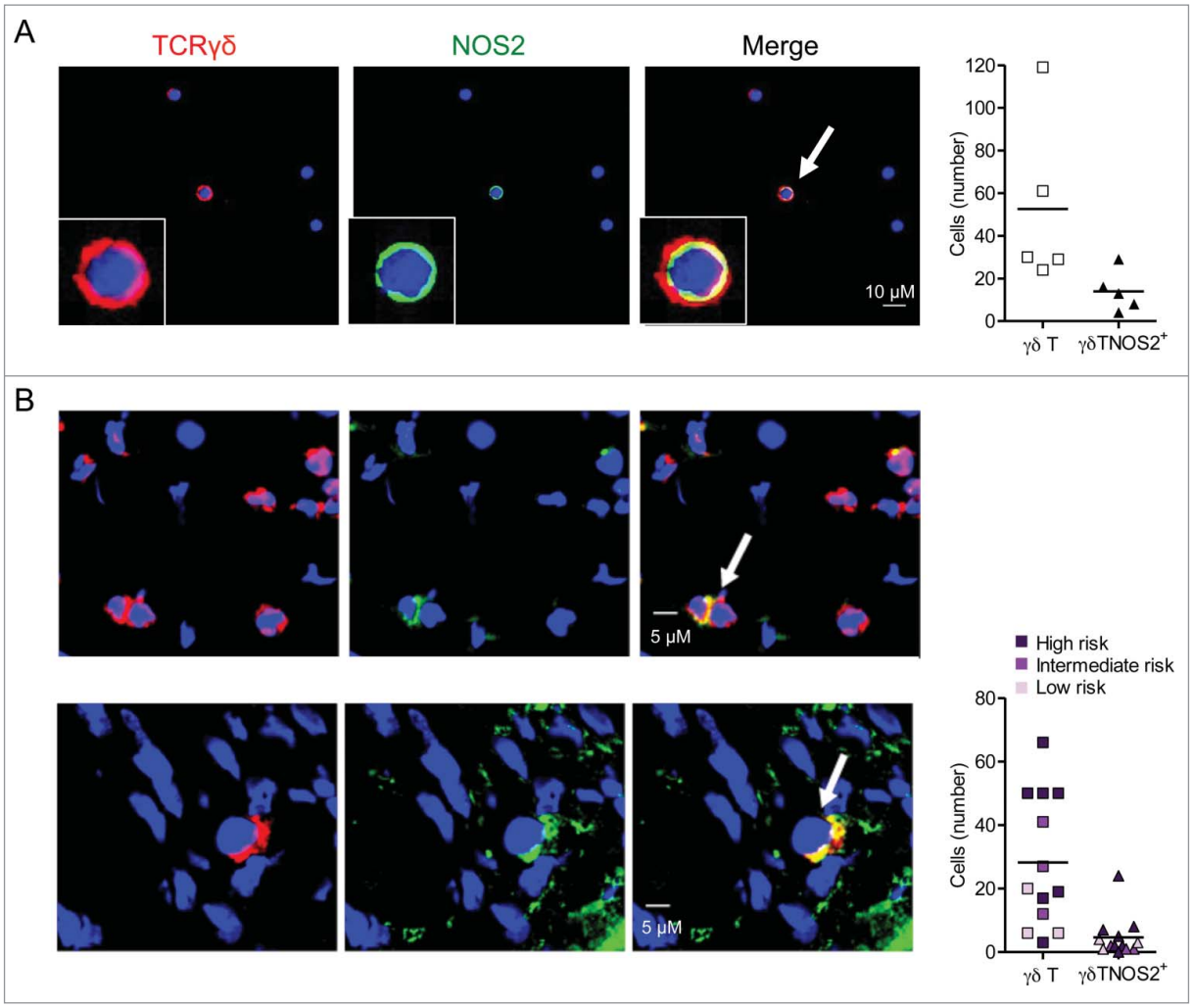

Figure 5. $\gamma\delta$ Tcells infiltrating mouse and human melanoma are able to express NOS2. (A) Representative confocal microscopy images showing $\gamma\delta$ T cells positive for NOS2 from cells derived from TdLNs of Ret mice and stained with antibodies to TCR $\gamma\delta$ (red), NOS2 (green) and counterstained with DAPI (blue). Bars 10 μM. 40 X objective (left). Quantification of $\gamma\delta$ T cells and $\gamma\delta$ T cells positive for NOS2 from 500 to 1,500 cells (right). Experiments were performed five times. (B) Representative digital microscopy images of 7 μm sections from frozen biopsies of human primary melanoma (patient 14 and 12, respectively). Sections were stained with antibodies to TCR $\gamma\delta$ (red) and NOS2 (green). Nuclei were counterstained with DAPI (blue). Bars 5 μM. 40 X objective (left). Quantification of $\gamma\delta$ T cells and $\gamma\delta$ T cells positive for NOS2 in 13 patients with detected $\gamma\delta$ T cells (right). Patients were divided into three groups with low, intermediate or high risk of disease's relapse according to Breslow thickness. Arrows indicate NOS2-expressing $\gamma\delta$ T cells.

by $\gamma\delta$ T cells. $\gamma\delta$ T cells were present in 13 out of 14 studied primary melanoma, but less abundant (+) in the low risk subgroup than in the two other groups. Three patients (# 4, 5 and 6) with a relatively thin melanoma had a primary tumor with an abundant infiltrate of $\gamma\delta$ T cells and did not experience a relapse of the disease after a mean follow up period of more than 4.5 y. On the contrary, $\gamma\delta$ T cells were abundant (+++) in the four patients with progressive disease except for patient 11 (where they were not detected). These results indicate that $\gamma\delta$ T cells infiltrate increases with primary melanoma progression (Table S2). Interestingly, we detected NOS2 positive $\gamma\delta$ T cells *in situ* in 12 out of the 13 primary melanomas (Table S2), as exemplified for patients 12 and 14 (the only patient with disseminated melanoma at diagnosis), respectively (Fig. 5B). In accordance with observation in mouse model, we found that 18% of $\gamma\delta$ T cells are positive for NOS2 in human primary melanoma (Fig. 5B). A larger series of patients has to be studied in order to determine whether or not these NOS2$^+$ $\gamma\delta$ T cell infiltrates have a prognostic value in clinical practice.

Discussion

In this study, we show that NOS2 promotes pro-tumor properties of $\gamma\delta$ T cells. In particular, NOS2 favors IL-17 production by $\gamma\delta$ T cells that leads to the recruitment of PMN-MDSCs and subsequently to metastasis formation. As $\gamma\delta$ T cells from WT mice already display a higher capacity to produce IL-17 than their counterparts in NOS2KO mice at steady state, our data suggest that NOS2 predetermines $\gamma\delta$ T cell polarization toward a pro-tumor phenotype

Global NOS2 expression has been associated with a poor prognosis in human cutaneous[21,22] as well as uveal[23] melanoma, but the mechanisms by which NOS2 is involved in tumor escape remains poorly explored. In Ret mice with a NOD genetic background, we have shown that the rapid tumor cell dissemination strongly correlates with a reduced dectin-1 expression on myeloid cells that is prevented by NOS2 inactivation.[24] Here, we observed that RetNos2KO mice with C57Bl/6J genetic background survived better than Ret mice owing to the

significant delay of tumor cell dissemination, despite a comparable primary tumor incidence in 6-mo-old animals. Our previous demonstration supported the key contribution of PMN-MDSCs in tumor cell dissemination in the Ret model.[16] The inhibition of metastasis formation in RetNos2KO mice could thus be explained, at least in part, by the poor accumulation of PMN-MDSCs at the primary tumor site when NOS2 is genetically inactivated.

Here, we demonstrate the role of NOS2 in promoting γδ17 cells with pro-tumor functions. Our results support the hypothesis that γδ17 cells from NOS2-competent Ret mice recruit PMN-MDSCs and induce angiogenesis, *via* triggering production of KC plus G-CSF and VEGF, respectively, overall favoring tumor cell dissemination. Thus, the mechanisms downstream IL-17 produced by γδ T cells in the Ret melanoma model are consistent with those reviewed in ref.[2]. Indeed, γδ17 cells promote directly, or via cancer cell stimulation, the recruitment, expansion, differentiation and survival of PMN-MDSCs both in mouse models of hepatocellular carcinoma[18] and breast cancer,[17] and in human colorectal cancer.[19] In 2015, Coffelt et al. demonstrated that γδ T cell-derived IL-17 induced the G-CSF signaling cascade required for PMN-MDSCs expansion.[17] Wu et al. showed that γδ17 cells produced interleukin 8—the human equivalent of murine KC—to attract MDSCs in human colorectal cancer.[19] Moreover, Wakita et al. indicated that γδ17 cells promote angiogenesis via induction of VEGF secretion.[25]

As γδ17 cells may exert antitumor functions,[5-7,26] we decided to directly investigate the role of γδ T cells in our model. Their pro-tumor properties were evidenced by the significant delay in metastasis incidence in Ret mice lacking γδ T cells. The role of γδ T cells was previously assessed in the widely used B16-F0 or B16-F10 melanoma transplantable models. Some studies highlight a protective role of γδ T cells in melanoma,[27-29] whereas other reports show that γδ T cells promote melanoma progression[30,31] or have any effects on lung foci formation.[32] Transplantable models could provoke an inflammatory environment subsequently modulating tumor-specific immune responses that could explain some of these controversial results.

NOS2 is expressed by a large range of cells and thus acts in an autocrine or paracrine manner. Here, we provide the first evidence that γδ T cells infiltrating either human or mouse primary melanoma produce NOS2. We predict a deleterious role of autocrine NOS2 by γδ T cells in cancer responses due to the promotion of γδ17 cell subset in Ret mice compared to RetNos2KO mice. However, NOS2 inducers in melanoma-infiltrating γδ T cells remain to identify. NOS2 expression was first described in myeloid cells exposed to pro-inflammatory factors (such as IFNγ and lipopolysaccharide).[33] TCR triggering also induces NOS2 in primary $CD4^+$ αβ T lymphocytes.[10,11] We found significant levels of IL-1β and IL-6 within the primary tumor of Ret mice. These cytokines, in combination with IL-23 and tumor growth factor-β (TGF-β), are known to promote γδ17 cell polarization.[19,34] IL-1β and IL-6 have been recently identified as NOS2 inducers in mouse macrophages[35] and in newly generated plasma cells,[36] respectively. The combination of IL-1β and IL-6 is also known to optimize *Nos2* transcription in Th17 cells.[11] We thus hypothesize that IL-1β, IL-6 and/or TCR triggering induce NOS2 in tumor-infiltrating γδ T cells, which in turn triggers their IL-17 expression and subsequently KC, G-CSF and VEGF production by γδ17 cell themselves, and/or other cell populations present in the tumor microenvironment.

To date, studies investigating the role of NOS2 in the context of cancer have mainly focused on NOS2 expressed by tumor cells or myeloid cells. Our data highlight for the first time that γδ T cells infiltrating primary tumors are a source of NOS2 both in human melanoma and in our murine melanoma model. Our study suggests NOS2 as a new intrinsic factor involved in the expansion of IL-17-producers tumor-promoting γδ T cells. As γδ T cell-based cancer immunotherapies are currently under investigation, our results further substantiate the importance of evaluating γδ T cell polarization based on NOS2 expression before their use in clinical trials.

Materials and methods

Mice

C57BL/6J (designated as WT) mice were purchased from Harlan and Jackson Laboratories. C57BL/6J *Nos2*$^{-/-}$ (designated as Nos2KO) mice were provided by Dr H-J Garchon (INSERM U1173, University of Versailles Saint-Quentin, Montigny-le-Bretonneux, France). WT and Nos2KO mice were used between 6 to 12 weeks of age. MT/ret$^{+/-}$ transgenic mice (called Ret later) that were on the C57BL/6J background expressed heterozygously the human RET oncogene. Ret mice were crossed with mice deficient for Nos2 or γδ T cells (γδKO mice provided by Dr P Pereira (Pasteur Institute, Paris, France)) to obtain RetNos2KO and Retγδ KO mice. RetNos2KO and Retγδ KO mice were compared to their own Ret mice littermates. Clinical signs of mice were assessed twice a month. Two weeks to 7-mo-old mice were used for experiments. Mice were sacrificed at indicated times or when considered moribund (prostrated, bristly, skinny). All mice were maintained in our animal facility under specific pathogen-free conditions.

Human samples

Cutaneous primary melanoma samples were obtained from patients at stages *in situ* to IV of the disease and were collected in two hospitals (Cochin and Bichat Hospitals, Paris, France). Patients were included if the size of the primary tumor was large enough to allow both an adequate pathological analysis and to spare a fresh tumor sample for the research program. Altogether 14 primary melanomas were collected from patients, nine males and five females, with a mean age of 67 y (30 to 92 y). Sites of primary melanoma were, respectively, the trunk for six patients, the limbs for five patients and the face for three patients. Mean Breslow thickness was 5.49 mm (0 to 20 mm). Clinical stages at initial diagnosis are indicated in Table S2. Three patients in the high risk group (melanoma > 3 mm) experienced a relapse of the disease and another patient had disseminated melanoma at initial diagnosis. Three of these four patients died of melanoma whereas the latter is alive with disease (AWD).

Melanoma cell lines and tumor inoculations

The B16-F10 melanoma cell line (called B16 later) provided by Prof. I. Fidler (The University of Texas M. D. Anderson Cancer Center, Houston, TX) was cultured in RPMI 1640+Glutamax

(Gibco®), 10% FCS, 100 U mL^{-1} penicillin and streptomycin at 37°C, 5% CO_2. Tumor cells were inoculated s.c. (10^6 cells) into the flank or i.v. (10^5 or 10^6 cells) of WT or Nos2KO mice. Tumors were removed 2 weeks after tumor challenge.

Single-cell suspension procedures

LNs were mechanically dissociated, homogenized, and passed through a 100 μM cell strainer in 5% (vol/vol) FCS and 0.5% EDTA in phosphate-buffered saline (PBS). Tumors were mechanically dissociated and digested with 1 mg mL^{-1} collagenase D and 0.1 mg mL^{-1} DNase I for 20 min at 37°C.

Culture of $\gamma\delta$ T cells

$\gamma\delta$ T cells were sorted from pLNs. $CD4^+$, $CD8^+$ and $CD19^+$ cells were depleted using Dynabeads® (Invitrogen) before a negative sorting using Aria III cytometer (BD Biosciences). Highly purity of $\gamma\delta$ T cells with untouched TCR was obtained. $\gamma\delta$ T cells were cultured in RPMI 1640+Glutamax (Gibco®) with 10% FCS, 100 U mL^{-1} penicillin and streptomycin, 10 mM HEPES, 1 mM sodium pyruvate, non-essential amino acids, 50 μM 2-mercaptoethanol in 96 well plates at 37°C, 5% CO_2. Cells were cultured on plate-bound with 0.1 μg mL^{-1} anti-CD3ε (145-2C11) and 10 μg mL^{-1} anti-CD28 (37.51) (both from eBioscience).

Antibodies

Following anti-mouse Abs were used for flow cytometry: FITC—conjugated anti-Ly6G (1A8), anti-B220 (RA3-632), anti-IFNγ (XMG1.2) and anti-Vγ4 (UC3-10A6), PE—conjugated anti-δTCR (GL3) and anti-NK1.1 (PK136), APC- conjugated anti-CD45.2 (104), anti-CD11b (M1/70) and anti-Vγ1 (2.11), PerCP-Cy5.5—conjugated anti-CD3 (145-2C11), anti-βTCR (H57-597), and anti-CD45.2 (104), Pacific Blue-conjugated anti-$CD4^+$ (RM4-5), V450-conjugated anti-Ly6C (AL-21) and anti-CD27 (LG.3A10), PE-Cy7-conjugated anti-CD11c (HL3), APC-H7-conjugated anti-CD8 (53-6.7), Alexa Fluor 700-conjugated anti-IL-17A (TC11-18H10). Abs were purchased from BD Biosciences except anti-CD11b, anti-B220 and anti-βTCR from eBioscience.

Following purified anti-mouse Abs were purchased from eBioscience and used to deplete cells before $\gamma\delta$ T cells cell sorting: anti-CD19 (eBio1D3), anti-$CD8^+$ (53–6.7), anti-$CD4^+$ (GK 1.5).

Microscopy was performed using primary Abs; rabbit anti-human NOS2 (SP126, ThermoFisher Scientific), mouse anti-human $\gamma\delta$ TCR (11F2, BD Biosciences), biotin hamster anti-mouse $\gamma\delta$ TCR (GL3, BD Biosciences) and rabbit anti-mouse NOS2 (Calbiochem). Alexa fluor 488-conjugated goat anti-rabbit (Jackson immuno research), Alexa fluor 546-conjugated goat anti-mouse (Life Technologies) and PE-conjugated streptavidine (BD Biosciences) were used as secondary Abs.

Cell staining and flow cytometry

Surface staining was performed by incubating cells on ice, for 20 min, with saturating concentrations of labeled Abs in PBS, 5% FCS and 0.5% EDTA. Mouse cell-staining reactions were preceded by a 15-min incubation with purified anti-CD16/32 Abs (FcγRII/III block; 2.4G2) obtained from hybridoma supernatants. Intracellular cytokine staining were performed after stimulation of single-cell suspensions with Phorbol 12-myristate 13-acetate (PMA) (50 ng mL^{-1}) (Sigma), ionomycin (0.5 μg mL^{-1}) (Sigma) and 1 μL mL^{-1} Golgi Plug™ (BD Biosciences) for 4 h at 37°C 5% CO_2. Cells were incubated with Live/Dead Blue stain (Invitrogen), according to the manufacturer protocol prior to Ab surface staining. Then, intracellular staining was performed using Cytofix/Cytoperm™ kit (BD biosciences) following the manufacturer's instructions. Data files were acquired and analyzed on LSRII using Diva software (BD Biosciences).

Microscopy

For mouse staining, haematopoietic cells were magnetically sorted from primary tumors of Ret mice with anti-$CD45^+$ MicroBeads (Miltenyi Biotec). Then, haematopoietic cells were centrifuged onto a microscope slide using Cellspin 1 (Tharmac). For human staining, sections of 7 μm thickness were obtained from frozen biopsy of melanoma. Non-specific reactivity was performed with incubation of PBS, 1% BSA for 20 min at room temperature (RT). Primary Abs were incubated 1 h at RT. Then, slides were washed in PBS, 1% BSA before being incubated with the appropriate conjugated secondary Ab for 30 min at RT. Finally, nuclei were labeled with DAPI and slides were mounted in Vectashield mounting medium (Vector Labs). Images were acquired using a confocal imaging microscope (Leica DMI6000) using 40X or 100X objectives or with an automated high-resolution scanning system (Lamina™, PerkinElmer) with 40X objective. Acquisitions were performed with Metamorph software and images were analyzed with ImageJ and Panoramic Viewer (3DHISTECH).

Lysis assays

Cytotoxicity capacity of $\gamma\delta$ T cells was explored using the xCELLigence System (Roche).[37] The system dynamically measures electrical impedance across microelectrodes integrated on specific 96 well plates (E-plates). The impedance values, expressed as cell index (CI), provide quantitative information of cell adhesion, number and morphology. $\gamma\delta$ T cells were sorted from pLNs from Ret and RetNos2KO mice, then cultured for 48 h with 10 μg mL^{-1} anti-CD28, 15 U mL^{-1} rIL-2 and with 0.1 μg mL^{-1} anti-CD3ε (stimulated $\gamma\delta$ T cells) or without (non-stimulated $\gamma\delta$ T cells). 5×10^4 B16 cells were seeded into wells of E-plates. After adhesion of tumor cells (4 h), 2×10^4 $\gamma\delta$ T cells were added to the cultures. Tumor cell proliferation was dynamically monitored every 30 min for up 4 h. Results are expressed as percentage of lysis determined from CI normalized with RTCA Software (nCI): $[(nCI\ (B16)_{t = 4h} - nCI\ (B16 + \gamma\delta\ T\ cell)_{t = 4h} / nCI\ (B16)_{t = 4h})] \times 100$.

Protein quantifications

Quantitative determination of IFNγ, IL-12, IL-10, TNF-α, VEGF, G-CSF, KC, IL-1β, IL-6 and IL-17 concentrations were performed in aqueous humor using kits from R&D Systems or Meso Scale Discovery according to supplier instructions. For

aqueous humor collection, primary tumors were mechanically dissociated in 150 μL of PBS and frozen until use.

Statistics

Data are expressed as mean ± SEM. The significance of differences between two series of results was assessed using the Mann–Whitney test. Comparison between survival or incidence curves was performed using Mantel-Cox log-rank test. Linear correlations were evaluated with Pearson test. ($^{*}p < 0.05$; $^{**}p < 0.01$; $^{***}p < 0.001$). All statistical analyses were performed using Prism 5 software (GraphPad).

Study approval

Mice experiments were carried out in accordance with the guidelines of the French Veterinary Department and were approved by the Paris-Descartes Ethical Committee for Animal Experimentation (decision CEEA34.AB.038.12).

The study protocol was approved by the ethics committee CPP Ile de France III (N° Am5937-3-2834) (EUDRACT 2010-A00838-31) and the study was performed according to the Declaration of Helsinki Principles. Patients who had to be treated surgically for a primary melanoma were informed of the objectives of the study and signed a written consent before inclusion.

Disclosure of potential conflicts of interest

No potential conflicts of interest were disclosed.

Acknowledgments

We are grateful to H-J. Garchon (Inserm U1173, University of Versailles Saint-Quentin, Montigny-le-Bretonneux, France) and P. Pereira (Pasteur Institute, Paris, France) who provide us mice deficient for Nos2 and $\gamma\delta$ T cells. J. Cherfils-Vicini, V. Molinier-Frenkel, Y. Richard, F. Castellano and N. Bercovici for critical review of the manuscript. We thank E. Donnadieu for advices on microscopy experiments, B. Lucas for helpful discussions. We acknowledge the Cochin cytometry and Immunobiology facility, the Histology and Immunostaining facility, the Animal core facility. We thank F. Boitier, N. Kramkimel, E. Maubec and J. Chanal for patient recruitment, patients who gave their consent to participate to this study, and C. Auger and D. Bourgeois from URC Paris Center who contributed to the immumela project.

Funding

This work was supported by the SILAB Jean Paufique foundation and the French Society of Dermatology. L. Douguet was supported by the "Ligue 520 contre le Cancer" and Paris VII University. A. Prevost-Blondel's team is supported by Fondation ARC and Comite "Ile de France" Ligue contre le Cancer.

Author contributions

L.D., L.B., R.L., and L.L. did experiments; L.D., and A.P.B. designed the study with the help of M.K., and M.F.A. and L.D., and A.P.B. wrote the manuscript; and all authors critically reviewed the manuscript.

References

1. Girardi M, Oppenheim DE, Steele CR, Lewis JM, Glusac E, Filler R, Hobby P, Sutton B, Tigelaar RE, Hayday AC. Regulation of cutaneous malignancy by gammadelta T cells. Science 2001; 294:605-9; PMID:11567106; http://dx.doi.org/10.1126/science.1063916
2. Silva-Santos B, Serre K, Norell H. gammadelta T cells in cancer. Nat Rev Immunol 2015; 15:683-91; PMID:26449179; http://dx.doi.org/10.1038/nri3904
3. Gentles AJ, Newman AM, Liu CL, Bratman SV, Feng W, Kim D, Nair VS, Xu Y, Khuong A, Hoang CD et al. The prognostic landscape of genes and infiltrating immune cells across human cancers. Nat Med 2015; 21:938-45; PMID:26193342; http://dx.doi.org/10.1038/nm.3909
4. Lanca T, Silva-Santos B. The split nature of tumor-infiltrating leukocytes: Implications for cancer surveillance and immunotherapy. Oncoimmunology 2012; 1:717-25; PMID:22934263; http://dx.doi.org/10.4161/onci.20068
5. Ma Y, Aymeric L, Locher C, Mattarollo SR, Delahaye NF, Pereira P, Boucontet L, Apetoh L, Ghiringhelli F, Casares N et al. Contribution of IL-17-producing gamma delta T cells to the efficacy of anticancer chemotherapy. J Exp Med 2011; 208:491-503; PMID:21383056; http://dx.doi.org/10.1084/jem.20100269
6. Cheng M, Qian L, Shen G, Bian G, Xu T, Xu W, Hu S. Microbiota modulate tumoral immune surveillance in lung through a gammadeltaT17 immune cell-dependent mechanism. Cancer Res 2014; 74:4030-41; PMID:24947042; http://dx.doi.org/10.1158/0008-5472.CAN-13-2462
7. Takeuchi A, Dejima T, Yamada H, Shibata K, Nakamura R, Eto M, Nakatani T, Naito S, Yoshikai Y. IL-17 production by gammadelta T cells is important for the antitumor effect of mycobacterium bovis bacillus Calmette-Guerin treatment against bladder cancer. Eur J Immunol 2011; 41:246-51; PMID:21182095; http://dx.doi.org/10.1002/eji.201040773
8. Lo Presti E, Dieli F, Meraviglia S. Tumor-infiltrating gammadelta T lymphocytes: Pathogenic role, clinical significance, and differential programing in the tumor microenvironment. Front Immunol 2014; 5:607; PMID:25505472; http://dx.doi.org/10.3389/fimmu.2014.00607
9. Rei M, Pennington DJ, Silva-Santos B. The Emerging Protumor Role of gammadelta T lymphocytes: Implications for cancer immunotherapy. Cancer Res 2015; 75(5):798-802; PMID:25660949; http://dx.doi.org/10.1158/0008-5472.CAN-14-3228
10. Jianjun Y, Zhang R, Lu G, Shen Y, Peng L, Zhu C, Cui M, Wang W, Arnaboldi P, Tang M et al. T cell-derived inducible nitric oxide synthase switches off Th17 cell differentiation. J Exp Med 2013; 210:1447-62; PMID:23797094; http://dx.doi.org/10.1084/jem.20122494
11. Obermajer N, Wong JL, Edwards RP, Chen K, Scott M, Khader S, Kolls JK, Odunsi K, Billiar TR, Kalinski P. Induction and stability of human Th17 cells require endogenous NOS2 and cGMP-dependent NO signaling. J Exp Med 2013; 210:1433-445; PMID:23797095; http://dx.doi.org/10.1084/jem.20121277
12. Eyles J, Puaux AL, Wang X, Toh B, Prakash C, Hong M, Tan TG, Zheng L, Ong LC, Jin Y et al. Tumor cells disseminate early, but immunosurveillance limits metastatic outgrowth, in a mouse model of melanoma. J Clin Invest 2010; 120:2030-9; PMID:20501944; http://dx.doi.org/10.1172/JCI42002
13. Kato M, Takahashi M, Akhand AA, Liu W, Dai Y, Shimizu S, Iwamoto T, Suzuki H, Nakashima I. Transgenic mouse model for skin malignant melanoma. Oncogene 1998; 17:1885-8; PMID:9778055; http://dx.doi.org/10.1038/sj.onc.1202077
14. Lengagne R, Le Gal FA, Garcette M, Fiette L, Ave P, Kato M, Briand JP, Massot C, Nakashima I, Renia L et al. Spontaneous vitiligo in an animal model for human melanoma: role of tumor-specific CD8+ T cells. Cancer Res 2004; 64:1496-501; PMID:14973052; http://dx.doi.org/10.1158/0008-5472.CAN-03-2828
15. Gabrilovich DI, Ostrand-Rosenberg S, Bronte V. Coordinated regulation of myeloid cells by tumours. Nat Rev Immunol 2012; 12:253-68; PMID:22437938; http://dx.doi.org/10.1038/nri3175
16. Toh B, Wang X, Keeble J, Sim WJ, Khoo K, Wong WC, Kato M, Prevost-Blondel A, Thiery JP, Abastado JP. Mesenchymal transition and dissemination of cancer cells is driven by myeloid-derived suppressor cells infiltrating the primary tumor. PLoS Biol 2011; 9:e1001162; PMID:21980263; http://dx.doi.org/10.1371/journal.pbio.1001162

17. Coffelt SB, Kersten K, Doornebal CW, Weiden J, Vrijland K, Hau CS, Verstegen NJ, Ciampricotti M, Hawinkels LJ, Jonkers J et al. IL-17-producing gammadelta T cells and neutrophils conspire to promote breast cancer metastasis. Nature 2015; 522:345-8; PMID:25822788; http://dx.doi.org/10.1038/nature14282
18. Ma S, Cheng Q, Cai Y, Gong H, Wu Y, Yu X, Shi L, Wu D, Dong C, Liu H. IL-17A produced by gammadelta T cells promotes tumor growth in hepatocellular carcinoma. Cancer Res 2014; 74:1969-82; PMID:24525743; http://dx.doi.org/10.1158/0008-5472.CAN-13-2534
19. Wu P, Wu D, Ni C, Ye J, Chen W, Hu G, Wang Z, Wang C, Zhang Z, Xia W et al. gammadeltaT17 cells promote the accumulation and expansion of myeloid-derived suppressor cells in human colorectal cancer. Immunity 2014; 40:785-800; PMID:24816404; http://dx.doi.org/10.1016/j.immuni.2014.03.013
20. Ribot JC, deBarros A, Pang DJ, Neves JF, Peperzak V, Roberts SJ, Girardi M, Borst J, Hayday AC, Pennington DJ et al. CD27 is a thymic determinant of the balance between interferon-gamma- and interleukin 17-producing gammadelta T cell subsets. Nat Immunol 2009; 10:427-36; PMID:19270712; http://dx.doi.org/10.1038/ni.1717
21. Ekmekcioglu S, Ellerhorst J, Smid CM, Prieto VG, Munsell M, Buzaid AC, Grimm EA. Inducible nitric oxide synthase and nitrotyrosine in human metastatic melanoma tumors correlate with poor survival. Clin Cancer Res 2000; 6:4768-75; PMID:11156233
22. Massi D, Franchi A, Sardi I, Magnelli L, Paglierani M, Borgognoni L, Maria Reali U, Santucci M. Inducible nitric oxide synthase expression in benign and malignant cutaneous melanocytic lesions. J Pathol 2001; 194:194-200; PMID:11400148; http://dx.doi.org/10.1002/1096-9896(200106)194:2%3c194::AID-PATH851%3e3.0.CO;2-S
23. Johansson CC, Mougiakakos D, Trocme E, All-Ericsson C, Economou MA, Larsson O, Seregard S, Kiessling R. Expression and prognostic significance of iNOS in uveal melanoma. Int J Cancer 2010; 126:2682-9; PMID:19847812; http://dx.doi.org/10.1002/ijc.24984
24. Dabbeche-Bouricha E, Araujo LM, Kato M, Prevost-Blondel A, Garchon H-J. Rapid dissemination of RET-transgene driven melanoma in the presence of non-obese diabetic alleles: critical roles of Dectin-1 and Nitric-Oxide Synthase type 2. Oncoimmunology. 2015 Oct 29; 5(5):e1100793; PMID:27467912; http://dx.doi.org/10.1080/2162402X.2015.1100793
25. Wakita D, Sumida K, Iwakura Y, Nishikawa H, Ohkuri T, Chamoto K, Kitamura H, Nishimura T. Tumor-infiltrating IL-17-producing gammadelta T cells support the progression of tumor by promoting angiogenesis. Eur J Immunol 2010; 40:1927-37; PMID:20397212; http://dx.doi.org/10.1002/eji.200940157
26. Mattarollo SR, Loi S, Duret H, Ma Y, Zitvogel L, Smyth MJ. Pivotal role of innate and adaptive immunity in anthracycline chemotherapy of established tumors. Cancer Res 2011; 71:4809-20; PMID:21646474; http://dx.doi.org/10.1158/0008-5472.CAN-11-0753
27. Gao Y, Yang W, Pan M, Scully E, Girardi M, Augenlicht LH, Craft J, Yin Z. Gamma delta T cells provide an early source of interferon gamma in tumor immunity. J Exp Med 2003; 198:433-42; PMID:12900519; http://dx.doi.org/10.1084/jem.20030584
28. He W, Hao J, Dong S, Gao Y, Tao J, Chi H, Flavell R, O'Brien RL, Born WK, Craft J et al. Naturally activated V gamma 4 gamma delta T cells play a protective role in tumor immunity through expression of eomesodermin. J Immunol 2010; 185:126-33; PMID:20525896; http://dx.doi.org/10.4049/jimmunol.0903767
29. Lanca T, Costa MF, Goncalves-Sousa N, Rei M, Grosso AR, Penido C, Silva-Santos B. Protective role of the inflammatory CCR2/CCL2 chemokine pathway through recruitment of type 1 cytotoxic gammadelta T lymphocytes to tumor beds. J Immunol 2013; 190:6673-80; PMID:23686489; http://dx.doi.org/10.4049/jimmunol.1300434
30. Carmi Y, Rinott G, Dotan S, Elkabets M, Rider P, Voronov E, Apte RN. Microenvironment-derived IL-1 and IL-17 interact in the control of lung metastasis. J Immunol 2011; 186:3462-71; PMID:21300825; http://dx.doi.org/10.4049/jimmunol.1002901
31. Hao J, Dong S, Xia S, He W, Jia H, Zhang S, Wei J, O'Brien RL, Born WK, Wu Z et al. Regulatory role of Vgamma1 gammadelta T cells in tumor immunity through IL-4 production. J Immunol 2011; 187:4979-86; PMID:21987661; http://dx.doi.org/10.4049/jimmunol.1101389
32. Paget C, Chow MT, Duret H, Mattarollo SR, Smyth MJ. Role of gammadelta T cells in alpha-galactosylceramide-mediated immunity. J Immunol 2012; 188:3928-39; PMID:22412194; http://dx.doi.org/10.4049/jimmunol.1103582
33. Bogdan C. Nitric oxide and the immune response. Nat Immunol 2001; 2:907-16; PMID:11577346; http://dx.doi.org/10.1038/ni1001-907
34. Caccamo N, La Mendola C, Orlando V, Meraviglia S, Todaro M, Stassi G, Sireci G, Fournie JJ, Dieli F. Differentiation, phenotype, and function of interleukin-17-producing human Vgamma9Vdelta2 T cells. Blood 2011; 118:129-38; PMID:21505189; http://dx.doi.org/10.1182/blood-2011-01-331298
35. Bogdan C. Nitric oxide synthase in innate and adaptive immunity: an update. Trends Immunol 2015; 36(3):161-78; PMID:25687683; http://dx.doi.org/10.1016/j.it.2015.01.003
36. Saini AS, Shenoy GN, Rath S, Bal V, George A. Inducible nitric oxide synthase is a major intermediate in signaling pathways for the survival of plasma cells. Nat Immunol 2014; 15:275-82; PMID:24441790; http://dx.doi.org/10.1038/ni.2806
37. Lengagne R, Pommier A, Caron J, Douguet L, Garcette M, Kato M, Avril MF, Abastado JP, Bercovici N, Lucas B et al. T cells contribute to tumor progression by favoring pro-tumoral properties of intratumoral myeloid cells in a mouse model for spontaneous melanoma. PLoS One 2011; 6:e20235; PMID:21633700; http://dx.doi.org/10.1371/journal.pone.0020235